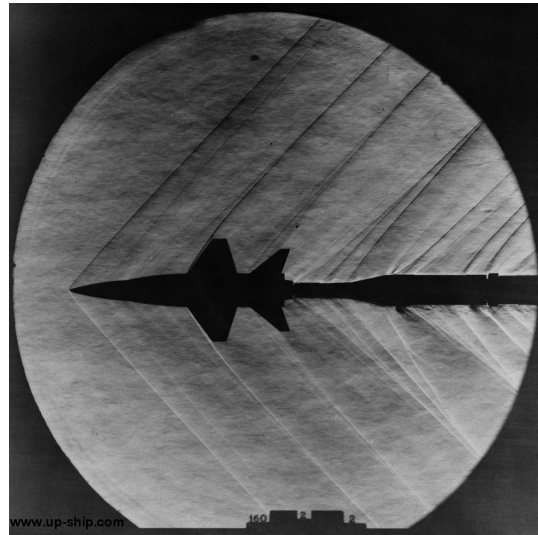


## Report

# Experimental Methods For Engineers

Background Oriented Schlieren (BOS)



**Maximilian Boosfeld**

**Michel Heusser**

**Kaspar Schlegel**

(November 2012)



# Contents

|   |            |
|---|------------|
| <b>Abstract</b>   | <b>iii</b> |
| <b>1 Introduction</b>   | <b>1</b>   |
| 1.1 Optical Density Measurements . . . . .                    | 1          |
| 1.2 Schlieren measurements, Examples Of Use . . . . .         | 1          |
| 1.3 Working Principle Of Synthetic Schlieren Method . . . . . | 2          |
| <b>2 Experimental Setup</b>                                   | <b>3</b>   |
| <b>3 Analysis Procedure</b>                                   | <b>5</b>   |
| 3.1 Imaging System . . . . .                                  | 5          |
| 3.2 Wedge calibration . . . . .                               | 6          |
| 3.3 Convection Cell . . . . .                                 | 6          |
| <b>4 Measurements And Results</b>                             | <b>8</b>   |
| 4.1 Wedge Experiment . . . . .                                | 8          |
| 4.2 Convection Cell . . . . .                                 | 8          |
| <b>5 Summary And Outlook</b>                                  | <b>12</b>  |
| 5.1 Recognized Shortcomings . . . . .                         | 12         |
| 5.2 Potential Improvements . . . . .                          | 12         |
| 5.3 Outlook And General Conclusion . . . . .                  | 12         |
| <b>Bibliography</b>   | <b>13</b>  |
| <b>A MATLAB Code</b>  | <b>14</b>  |

# List of Figures

|     |  |    |
|-----|--|----|
| 1.1 | Working Principle Optical Schlieren - <i>Source: [1]</i> . . . . .   | 1  |
| 1.2 | Working Principle Synthetic Schlieren - <i>Source: [1]</i> . . . . .                                       | 2  |
| 2.1 | Experimental Setup . . . . .   | 3  |
| 3.1 | Geometry Of The Optical Setup . . . . .  | 5  |
| 4.1 | Correlation Peaks And Wedge Calibration . . . . .  | 8  |
| 4.2 | Image Shifts Compared To Reference Image (left) And Calculation Quality Factor (right) At Time 1 . . . . . | 9  |
| 4.3 | Image Shifts Compared To Reference Image (left) And Calculation Quality Factor (right) At Time 2 . . . . . | 9  |
| 4.4 | Reference Image at $l = 175\text{mm}$ (No Heating) . . . . .   | 10 |
| 4.5 | Refraction (Left) And Temperature (Right) Distributions At Time 1  | 10 |
| 4.6 | Refraction (Left) And Temperature (Right) Distributions At Time 2  | 11 |

# Abstract

This experiment helps us to investigate and visualize different flow characteristics like density and temperature through analysis of the refraction index of a transparent liquid. In this experiment we made use of a camera and a noise-background. After having calibrated the measurements with the wedge experiment (measurement of the pixel deviation in the camera with known angle deviation of a certain probe lense) we measured the deviation of the noise background through a heated paraffin-filled probe. Through the mathematical relations between pixel deviation and light refraction were able to obtain very plausible temperature profiles (closely related to the refraction index) at two different times of the heated convection cell filled with paraffin.

# Chapter 1

## Introduction

Schlieren photography is a powerful technique to visualize density and temperature variations in flows. It was invented 1864 by August Toepler to examine supersonic motion. Schlieren technology is based on the principle of light being bent by refractive index variations due to the different propagation speed of light.  $n = \frac{c_0}{c}$

### 1.1 Optical Density Measurements

The classical Schlieren technology consists of a point source of illumination, several lenses, a test section and a camera as depicted in Figure 1.1.

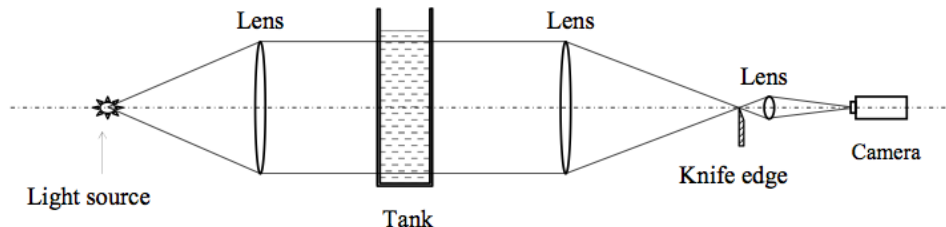


Figure 1.1: Working Principle Optical Schlieren - *Source: [1]*

In the test section the collimated light beam is distorted by density gradients in the fluid. Distortions create spatial variations in light intensity and the "knife" stops the rays deviated from parallelism. Though all Schlieren technologies have the huge advantage of being non-invasive there are several difficulties to this technique. First of all the experimental setup of positioning the lenses is complicated, sensitive to disturbances and fairly expensive. Furthermore the emitted light from a single-point source is limited as well as the size of lenses. Finally direct quantitative analysis remains difficult due to the fact that all information is encoded in brightness and no absolute reference is available.

### 1.2 Schlieren measurements, Examples Of Use

Background Oriented Schlieren (BOS), first introduced in the late 1990's, is a much simpler technique of the larger field of Synthetic Schlieren. Just as the optical Schlieren method it is commonly used for two-dimensional flow visualizations of

temperature and density changes in several fields, such as fluid mechanics, ballistics, heat exchange through convection, as well as observing the propagation and mixing behavior of gases. Latest developments of this technique even allow precise quantitative visualization of fluid flows, coupling the refractive index with flow properties.

### 1.3 Working Principle Of Synthetic Schlieren Method

As mentioned earlier the setup for the Synthetic Schlieren technique is much simpler than one of the Optical Schlieren method. Beams from the diffuse light source pass through a mask and are captured by a digital camera as illustrated in Figure 1.2. A reference picture (without test section) is compared with one containing the test section.

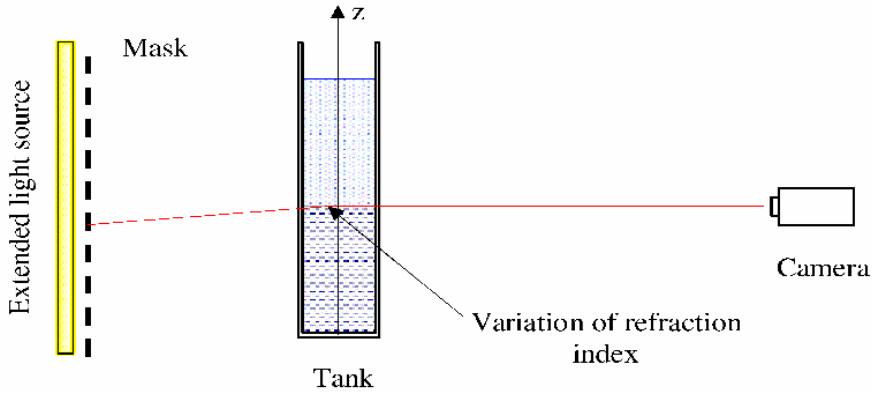


Figure 1.2: Working Principle Synthetic Schlieren - *Source: [1]*

The improvements are obvious. No expensive mirrors, lenses and no single-point source of light is needed. The technique of Background Oriented Schlieren (BOS) is even simpler. Instead of an extended light source and a mask only a random background pattern is needed.

To derive from optical distortions to temperature or density variations, a relation between refractive index and fluid properties is needed. The "Gladstone-Dale" relationship

$$n - 1 = K \cdot \rho = K \cdot \frac{p}{RT} \quad (1.1)$$

provides such link for gases. The empirical relationship for paraffin oil used in the experiment is shown below.

$$n(T) = 1.48 - 0.00036 \cdot T(^{\circ}C) \quad (1.2)$$

## Chapter 2

# Experimental Setup

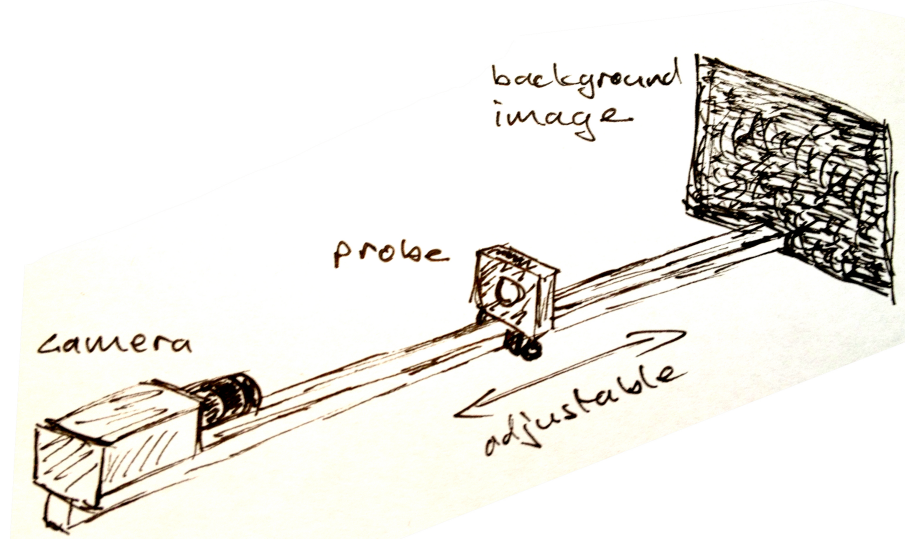


Figure 2.1: Experimental Setup

The experimental setup consists of a camera, an adjustable fitting for the probe and a background image. The setup is drawn in Figure 2.1. The camera is controlled by computer and has only medium resolution because high resolution is not required. The background image is a random black and white pattern, where no repetitions of the pattern are allowed. The distance between the background image and the camera is held constant, while the distance between the probe and the camera (and therefore as well the distance between the probe and the background image) can be adjusted.

In the calibration experiment, a wedge prism with a known deflection angle of  $1^\circ$  is used as probe. First of all, a reference picture without probe is captured. Afterwards a series of 16 pictures at 16 different positions is made. This is subsequently

processed in MATLAB and a calibration factor can be derived.

In the flow cell experiment, the probe is a convection cell. This convection cell has paraffin oil as fluid and on one side, an electric heating is attached and on the other side a heat conducting material. Again, a reference picture with the flow cell on it (when the electrical heating is not activated) is taken. The heating is then activated and after some time another picture is captured. With MATLAB and the data from the previous calibration measurement, the post processing is made and the gradient field of the temperature can be visualized.

# Chapter 3

## Analysis Procedure

### 3.1 Imaging System

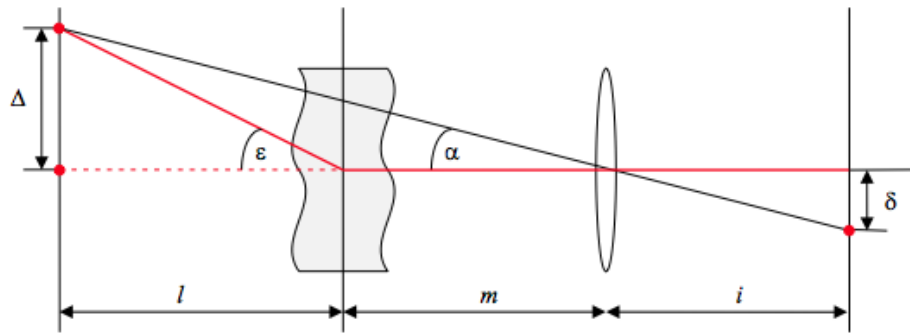


Figure 3.1: Geometry Of The Optical Setup

From the geometry of the optical setup shown in figure 3.1, we can derive the following relations:

$$\tan(\epsilon) = \frac{\Delta}{l} \quad (3.1)$$

$$o = l + m \quad (3.2)$$

$$\tan(\alpha) = \frac{\Delta}{o} = -\frac{\delta}{i} \quad (3.3)$$

The lens equation is as well given by:

$$\frac{1}{o} + \frac{1}{i} = \frac{1}{f} \quad (3.4)$$

Combining equations 3.1, 3.2, 3.3 and 3.4 using the limit for large image imaging distances  $o \gg f$ , we obtain equation 3.5:

$$\delta \approx \frac{f}{1 + \frac{m}{l}} \tan(\epsilon) \quad (3.5)$$

which is the image displacement on the sensor surface.

For the cumulative deflection vector field, we use equation 3.6 (with  $l \rightarrow \infty$ ):

$$\vec{\delta}(x, y) \approx -f \cdot \tan(\epsilon) = -\frac{f}{n_0} \int_{-\infty}^{+\infty} \nabla n_1(x, y, z) dz \quad (3.6)$$

### 3.2 Wedge calibration

With MATLAB, we read in the images and crop an area in the middle of the wedge prism. These cropped images are then auto-correlated to the reference image and the positions of the correlation peaks are compared. Therefrom we obtain the deflection (=image shifts). In the following equation 3.7, the deflection  $|\delta_{pix}^{1^\circ}(l)|$  for the wedge prism is derived:

$$|\delta_{pix}^{1^\circ}(l)| = \kappa \frac{lf}{o} \tan(1^\circ) [pixel] \quad (3.7)$$

Where  $\kappa$  is the pixel size ( $[\kappa] = \frac{pixels}{m}$ ),  $l$  the distance from the object to the background image,  $f$  the focal length of the camera and  $o$  the distance between camera and background image.

For subsequent measurement we can use the scaling relation:

$$\frac{\tan(\vec{\epsilon})}{\tan(1^\circ)} = -\frac{\vec{\delta}_{pix}}{|\delta_{pix}^{1^\circ}(l)|} \quad (3.8)$$

Where  $\vec{\epsilon}$  is the deflection angle.

### 3.3 Convection Cell

A given MATLAB script 'SimplePIV' calculates the image shifts. The refractive index gradient can be calculated with Equation 3.9, which is simplified with the scaling relation from Equation 3.8:

$$\vec{\nabla}n \approx \frac{n_0}{L} \tan(\vec{\epsilon}) = -\frac{n_0}{L} \tan(1^\circ) \frac{\vec{\delta}_{pix}}{|\delta_{pix}^{1^\circ}(l)|} \quad (3.9)$$

where  $L$  is the length of the test cell (10 mm).

The refractive index gradient from 3.9 can then be integrated (with boundary conditions) to obtain the refractive index. In our experiment, we can use a provided MATLAB file 'IntegrateDisplacements' for the integration. The boundary condition is a constant refractive index on the right hand side of the flow cell (side without electrical heating). We can't use the direct displacements calculated before and

have to multiply it with a scaling factor  $\phi = \sigma \cdot \gamma$  where  $\sigma$  is the pixel scale factor ( $\sigma = [\frac{m}{pixel}]$ ) and  $\gamma$  the grid unit (i.e. the increment parameter in the 'SimplePIV' method with  $\gamma = \frac{pixel}{gridunit}$ ).

Finally, the temperature field can then be calculated with Equation 1.2. The MATLAB file can be seen in the Appendix.

## Chapter 4

# Measurements And Results

### 4.1 Wedge Experiment

The plot is shown in Figure 4.1. A linear relation can be seen. For the following measurement of the flow cell we can use the scaling relation 3.8 an read the value for  $|\delta_{pix}(1^\circ)|$  from the plot.

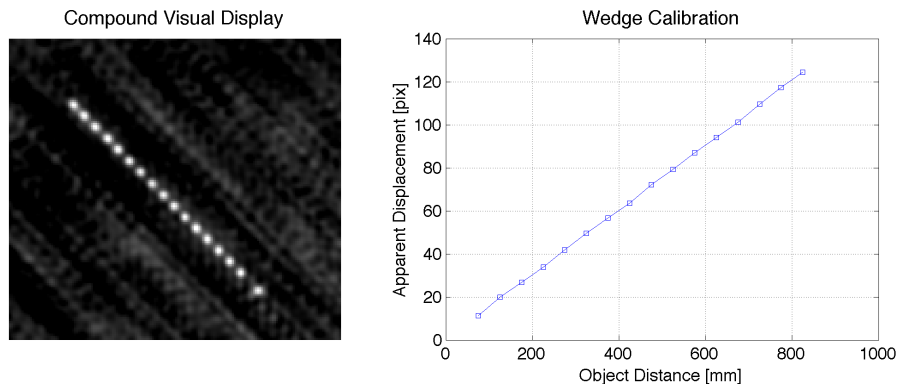


Figure 4.1: Correlation Peaks And Wedge Calibration

### 4.2 Convection Cell

After the Wedge Experiment is performed for the calibration of our experimental setup, we proceed to install the probe filled with paraffin. A reference picture was taken before turning on the heating wall on the probe. After turning on the heating system, two pictures were taken at different times whose temperature profile is going to be analysed. The measurements of the probe took place at distance  $l = 175\text{mm}$  from the reference background-screen. The reason of chosing one of the first distances on the probe-rail is to reduce the optical deviations.

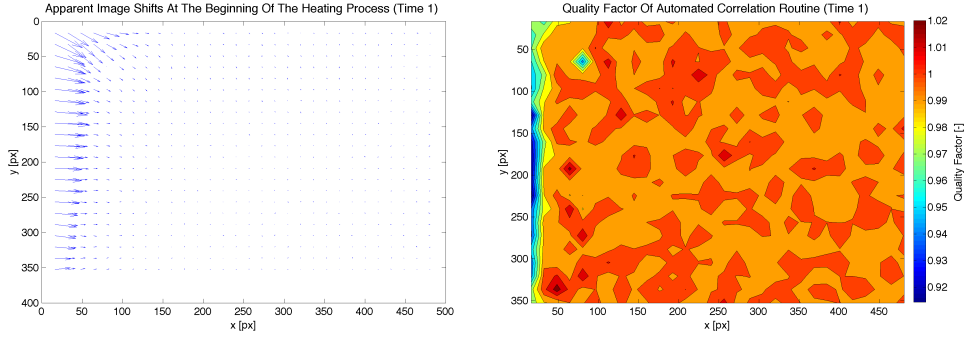


Figure 4.2: Image Shifts Compared To Reference Image (left) And Calculation Quality Factor (right) At Time 1

On the left side of Figures 4.2 and 4.3 we observe the field of image deviations of the heated probes compared to the reference unheated probe. We observe in both cases, that the image shifts are more prominent near the heating wall on the left. We also see in the picture taken at a previous time, that the areas further away from the heating source seem practically unaffected (no shift), whereas at the second picture the whole measured field is affected.

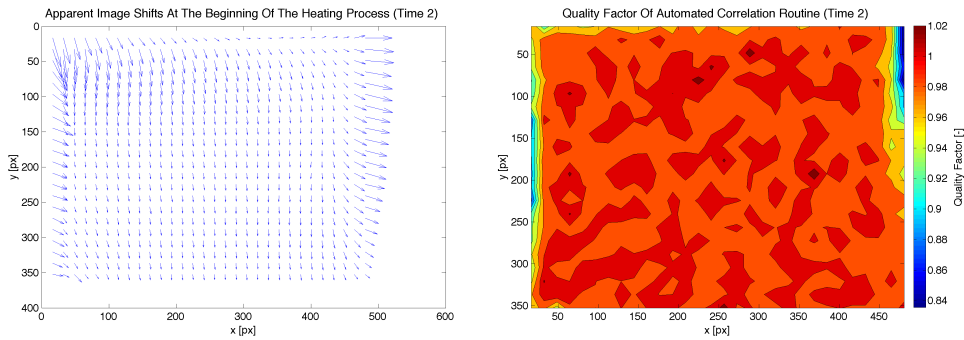


Figure 4.3: Image Shifts Compared To Reference Image (left) And Calculation Quality Factor (right) At Time 2

In the right part of Figures 4.2 and 4.3 we observe the quality (or reliability) of the calculation of the mentioned vector field of shifts. The value of the quality is centered around one, which is the best achievable quality. The rectangle in the pictures taken in consideration for the image analysis was chosen according to this quality, so that the shown results are reliable enough (here, between 1.02 and 0.84). The reason of the quality being lower on the sides is the irregularity of the image (blurriness) in those areas, as we can see in Figure 4.4.

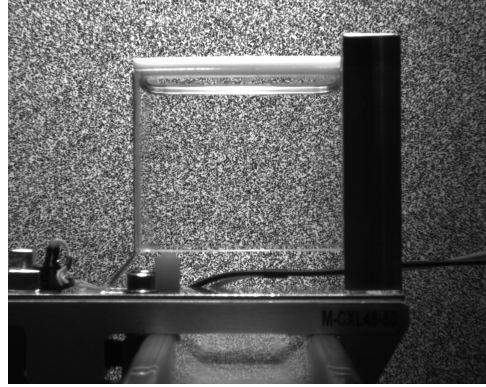


Figure 4.4: Reference Image at  $l = 175\text{mm}$  (No Heating)

From the relation 3.9 we see clearly that the shift-field shown above is actually proportional to the gradient of  $n$ . While solving the equation for  $n$  and then calculating  $T$ , or, in other words, calculating the refraction index and the temperature profile out of our image-shifting measurements we get Figure 4.5 for Time 1 and Figure 4.6 for Time 2. While comparing the corresponding image-shifting-field we see immediately the first mathematical consequence: The shifting vectors are perpendicular to the isopotential lines of  $n$  and  $T$ .

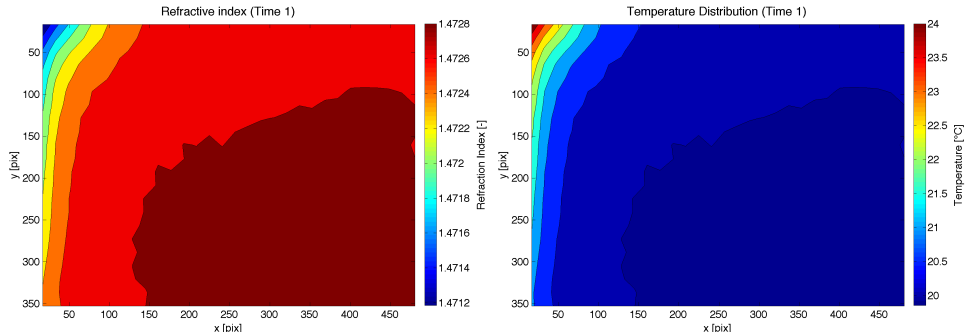


Figure 4.5: Refraction (Left) And Temperature (Right) Distributions At Time 1

Since the temperature and the defraction index are linearly related, the results look qualitatively similar. We will only discuss the temperature profile, since it's the main objective of this experiments. We observe how the temperature profile shows both thimes a higher temperature near the heating wall. As expected, the distribution of heat is less homogeneous throughout the  $x$ -axis at later times. Moreover, the paraffin has had more time to get heated and rise it's temperature peak ( $24^\circ\text{C}$  at Time 1 and  $30^\circ\text{C}$  at Time 2).

The reason that the temperature is highest on the top left an not along the whole heating wall is due to heat convection effects which drive the hotter paraffin to the top. That leads to the uneven heat distbution along the  $y$ -axis. With this we can understandwhy the gradient field of the image shifts (Figures 4.2 and 4.3) is steeper on the upper left part of the probe.

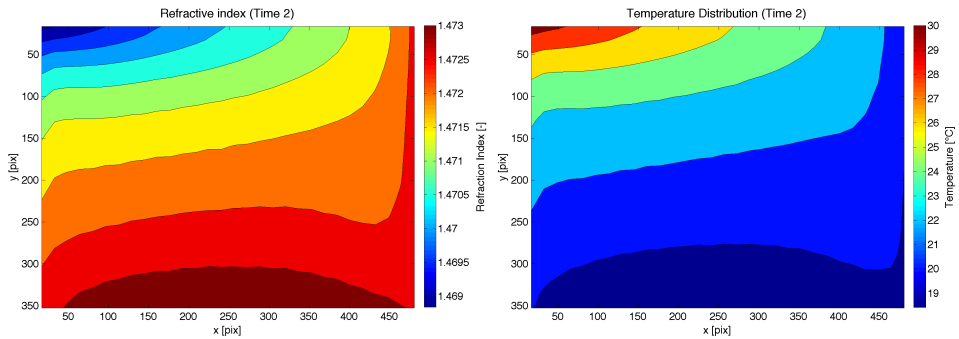


Figure 4.6: Refraction (Left) And Temperature (Right) Distributions At Time 2

# **Chapter 5**

## **Summary And Outlook**

### **5.1 Recognized Shortcomings**

One of the shortcomings that we could observe in this experiment is the size of the probe used. Although the wedge experiment for the calibration delivered very good results, the temperature fields could have delivered better results, specially on the edges, if the probe (and thus the area of analysis) would have been bigger. Also, the fact that the temperature field was only calculated for two different times, the results have little significance in terms of time. The camera having itself a curved lens, could have a certain effect on the results depending on how close the lens is to the probe. Ideally, the best results would be delivered by a camera with a high zoom, that is still far away from the probe. This would, of course require a higher quality lens and sensor to maintain the quality of the picture.

### **5.2 Potential Improvements**

The value of the results could be much higher if, for example, there was a bigger batch of analysed pictures at known times. In this case, more conclusions could be made about the properties of the heat distribution in paraffin.

### **5.3 Outlook And General Conclusion**

The method of the Schlieren Analysis taught us how so plausible and reliable results can be taken from such a simple setup (a camera and a background with noise). Of course there is the disadvantage of measuring fluids with high opacity. But this technique allows us, even to perform quality measures (with the help of MATLAB) only with equipment found home.

# Bibliography

- [1] LP Thomas, BM Marino, and SB Dalziel. Synthetic schlieren: determination of the density gradient generated by internal waves propagating in a stratified fluid. In *Journal of Physics: Conference Series*, volume 166, page 012007. IOP Publishing, 2009.

# **Appendix A**

## **MATLAB Code**

11/15/12 12:04 PM /Network/Serve.../bos\_schlieren.m 1/6

```
close all
clear all
clc

%%
%Wedge Calibration

% Einlesen der Bilder
r=imread('Referenz.tif');

a=imread('75.tif');
b=imread('125.tif');
c=imread('175.tif');
d=imread('225.tif');
e=imread('275.tif');
f=imread('325.tif');
g=imread('375.tif');
h=imread('425.tif');
i=imread('475.tif');
j=imread('525.tif');
k=imread('575.tif');
l=imread('625.tif');
m=imread('675.tif');
n=imread('725.tif');
o=imread('775.tif');
p=imread('825.tif');

% Wählen des Bildausschnittes
rect = [551, 377, 157, 142];

rs=imcrop(r,rect);

as=imcrop(a,rect);
bs=imcrop(b,rect);
cs=imcrop(c,rect);
ds=imcrop(d,rect);
es=imcrop(e,rect);
fs=imcrop(f,rect);
gs=imcrop(g,rect);
hs=imcrop(h,rect);
is=imcrop(i,rect);
js=imcrop(j,rect);
ks=imcrop(k,rect);
ls=imcrop(l,rect);
ms=imcrop(m,rect);
ns=imcrop(n,rect);
os=imcrop(o,rect);
ps=imcrop(p,rect);

% Korrelation
rc=normxcorr2(rs,r);

ac=normxcorr2(as,r);
bc=normxcorr2(bs,r);
cc=normxcorr2(cs,r);
dc=normxcorr2(ds,r);
ec=normxcorr2(es,r);
fc=normxcorr2(fs,r);
gc=normxcorr2(gs,r);
```

```
hc=normxcorr2(hs,r);
ic=normxcorr2(is,r);
jc=normxcorr2(js,r);
kc=normxcorr2(ks,r);
lc=normxcorr2(ls,r);
mc=normxcorr2(ms,r);
nc=normxcorr2(ns,r);
oc=normxcorr2(os,r);
pc=normxcorr2(ps,r);

%%

%Font sizes for figures
titlesize= 20;
axissize=18;
set(0,'DefaultAxesFontSize',axissize)

%Creation of figure of proper size
f0 = figure(1)
set(f0,'Position', [0 1000 1000 400])
set(f0,'PaperPositionMode','auto')% print() exports the same size as figures are shown
s01=subplot(1,2,1)
set(s01,'Position',[0.005 0.13 0.45 0.78])

%Compound plot
imshow(imcrop(rc+ac+bc+cc+dc+ec+fc+gc+hc+ic+jc+kc+lc+mc+nc+oc+pc,[590, 400, 157, 142]))
title('Compound Visual Display', 'FontSize',titlesize)

% Koordinaten der Korrelation
[maxval(1),maxind(1)]=max(rc(:));
[maxval(2),maxind(2)]=max(ac(:));
[maxval(3),maxind(3)]=max(bc(:));
[maxval(4),maxind(4)]=max(cc(:));
[maxval(5),maxind(5)]=max(dc(:));
[maxval(6),maxind(6)]=max(ec(:));
[maxval(7),maxind(7)]=max(fc(:));
[maxval(8),maxind(8)]=max(gc(:));
[maxval(9),maxind(9)]=max(hc(:));
[maxval(10),maxind(10)]=max(ic(:));
[maxval(11),maxind(11)]=max(jc(:));
[maxval(12),maxind(12)]=max(kc(:));
[maxval(13),maxind(13)]=max(lc(:));
[maxval(14),maxind(14)]=max(mc(:));
[maxval(15),maxind(15)]=max(nc(:));
[maxval(16),maxind(16)]=max(oc(:));
[maxval(17),maxind(17)]=max(pc(:));

% Pixelkoordinaten
size_cr=size(ac); % Grösse des cropped image, gleich für alle Bilder
for ii=1:17
    [rows(ii),cols(ii)]=ind2sub(size_cr,maxind(ii));
end

% Verschiebung in Pixelkoordinaten
for ii=1:16
    delta(ii,:)=norm([rows(ii+1)-rows(1),cols(ii+1)-cols(1)]);
end
```

```

end

% Calibration plot creation and exporting
s02 = subplot(1,2,2)
set(s02,'Position',[0.512 0.13 0.45 0.78])
distance=[75,125,175,225,275,325,375,425,475,525,575,625,675,725,775,825];
plot(distance,delta,'-s')
title('Wedge Calibration', 'FontSize',titlesize)
xlabel('Object Distance [mm]', 'FontSize',axissize)
ylabel('Apparent Displacement [pix]', 'FontSize',axissize)

grid on
print(f0,'/Network/Servers/mlh34-0.ethz.k
ch/Volumes/01_MXS_RAID/01_StudentData/mheusser/Dropbox/experimentellek
methoden/Schlieren Analysis/Report/pics/figure0','-dpng')

%%
% Flow cell
close all
clc

%Creation of figures of the proper size

f1 = figure(2); %Zeitpunkt 1
set(0,'DefaultAxesFontSize',axissize)
set(f1,'Position',[0 0 1600 600])
set(f1,'PaperPositionMode','auto')
f2 = figure(3); %Zeitpunkt 2
set(0,'DefaultAxesFontSize',axissize)
set(f2,'Position',[0 0 1600 600])
set(f2,'PaperPositionMode','auto')
f3 = figure(4); %Zeitpunkt 1
set(0,'DefaultAxesFontSize',axissize)
set(f3,'Position',[0 0 1600 600])
set(f3,'PaperPositionMode','auto')
f4 = figure(5); %Zeitpunkt 2
set(0,'DefaultAxesFontSize',axissize)
set(f4,'Position',[0 0 1600 600])
set(f4,'PaperPositionMode','auto')
subplotleftposition = [0.036 0.1 0.42 0.78];
subplotrightposition = [0.545 0.1 0.42 0.78];

%Cropping parameters
cropx = 382;
cropy = 268;
width = 500;
height = 370;

% Einlesen und croppen der Bilder
p_1=imread('175_p.tif'); %Zeitpunkt 1 (Eingeschaltet)
p_2=imread('175_p2.tif'); %Zeitpunkt 2 (Eingeschaltet)
rf=imread('Referenz_p.tif'); %Ausgeschaltet
rect2 =[cropx cropy width height];
% rect3 = [362.5100 2.5100 523.9800 641.9800]
% with control cell
% rect4 =[382.5100 267.5100 493.9800 369.9800]

```

```
% without control cell
p_1s=imcrop(p_1,rect2);
p_2s=imcrop(p_2,rect2);
rfs=imcrop(rf,rect2);

% Zeitpunkt 1
[x1,y1,u1,v1,q1,vld1]=SimplePIV(rfs,p_1s,32,8,16); %Calculation of gradient field

%Plot (Gradient Field 1)
set(0,'CurrentFigure',f1)
s11 = subplot(1,2,1);
set(s11,'Position',subplotleftposition)
quiver(x1,y1,-u1,-v1,2)
view(0,270)
title('Apparent Image Shifts At The Beginning Of The Heating Process (Time 1)', 'FontSize',titlesize)
xlabel('x [px]', 'FontSize',axissize)
ylabel('y [px]', 'FontSize',axissize)

%Plot (Quality Factor 1)
s12 = subplot(1,2,2)
set(s12,'Position',subplotrightposition)
%surf(x1,y1,q1)
contourf(x1,y1,q1)
c1 = colorbar;
set(get(c1,'YLabel'),'String','Quality Factor [-]', 'FontSize',axissize)
view(0,270)
title('Quality Factor Of Automated Correlation Routine (Time 1)', 'FontSize',titlesize)
xlabel('x [px]', 'FontSize',axissize)
ylabel('y [px]', 'FontSize',axissize)

% Zeitpunkt 2
[x2,y2,u2,v2,q2,vld2]=SimplePIV(rfs,p_2s,32,8,16);%Calculation of gradient field

%Plot (Gradient Field 2)
set(0,'CurrentFigure',f2)
s21 = subplot(1,2,1);
set(s21,'Position',subplotleftposition)
quiver(x2,y2,-u2,-v2,2)
view(0,270)
title('Apparent Image Shifts At The Beginning Of The Heating Process (Time 2)', 'FontSize',titlesize)
xlabel('x [px]', 'FontSize',axissize)
ylabel('y [px]', 'FontSize',axissize)

%Plot (Quality Factor 2)
s22 = subplot(1,2,2)
set(s22,'Position',subplotrightposition)
contourf(x2,y2,q2)
c2=colorbar;
set(get(c2,'YLabel'),'String','Quality Factor [-]', 'FontSize',axissize)
view(0,270)
title('Quality Factor Of Automated Correlation Routine (Time 2)', 'FontSize',titlesize)
xlabel('x [px]', 'FontSize',axissize)
```

```
ylabel('y [px]', 'FontSize', axisSize)

% Umrechnung in Gradient des Brechungsindexes
T_0 = 20;
n_0 = 1.48 - 0.00036*T_0;
L=10*10^(-3);
sigma= 50*10^(-3)/width; % [m/pix]
phi=16*sigma;

% Zeitpunkt 1

% Skalierung des Verschiebungsvektors mit Kalibrationsergebnis
gradnx1=-(n_0/L)*tan(2*pi/360)*(u1)/delta(3);
gradny1=-(n_0/L)*tan(2*pi/360)*(v1)/delta(3);

% Integration des Gradientenfeldes des Brechungsindexes
n1=IntegrateDisplacements(gradnx1*phi,gradny1*phi,NaN(height,1),n_0*ones*(height,1),NaN(1,width),NaN(1,width));

%Plot (Refraction index 1)
set(0,'CurrentFigure',f3)
s31 = subplot(1,2,1)
set(s31,'Position',subplotleftposition)
contourf(x1,y1,n1)
c3=colorbar;
set(get(c3,'ylabel'),'string','Refraction Index [-]', 'FontSize', axisSize)
view(0,270)
title('Refractive index (Time 1)', 'FontSize', titleSize)
xlabel('x [pix]', 'FontSize', axisSize)
ylabel('y [pix]', 'FontSize', axisSize)

% Umrechnung in Temperaturfeld
T1=(1.48-n1)./0.00036;

%Plot (Temperature Field 1)
s32=subplot(1,2,2)
set(s32,'Position',subplotrightposition)
contourf(x1,y1,T1)
c4=colorbar;
set(get(c4,'ylabel'),'string','Temperature [°C]', 'FontSize', axisSize)
view(0,270)
title('Temperature Distribution (Time 1)', 'FontSize', titleSize)
xlabel('x [pix]', 'FontSize', axisSize)
ylabel('y [pix]', 'FontSize', axisSize)

% Zeitpunkt 2
% Skalierung des Verschiebungsvektors mit Kalibrationsergebnis
gradnx2=-(n_0/L)*tan(2*pi/360)*(u2)/delta(3);
gradny2=-(n_0/L)*tan(2*pi/360)*(v2)/delta(3);

% Integration des Gradientenfeldes des Brechungsindexes (Grösse des Ausschnittes: x-Richtung 524 pixel, y-Richtung 370 pixel)
```

11/15/12 12:04 PM /Network/Serve.../bos\_schlieren.m 6/6

```
n2=IntegrateDisplacements(gradnx2*phi,gradny2*phi,NaN(height,1),n_0*ones<  
(height,1),NaN(1,width),NaN(1,width));  
  
%Plot (Refraction index 2)  
set(0,'CurrentFigure',f4)  
s41 = subplot(1,2,1)  
set(s41,'Position',subplotleftposition)  
contourf(x2,y2,n2)  
c5=colorbar;  
set(get(c5,'ylabel'),'string','Refraction Index [-]','FontSize',axissize)  
view(0,270)  
title('Refractive index (Time 2)', 'FontSize',titlesize)  
xlabel('x [pix]', 'FontSize',axissize)  
ylabel('y [pix]', 'FontSize',axissize)  
  
% Umrechnung in Temperaturfeld  
T2=(1.48-n2)./0.00036;  
  
%Plot (Temperature Field 2)  
s42= subplot(1,2,2)  
set(s42,'Position',subplotrightposition)  
view(0,270)  
contourf(x2,y2,T2)  
c6=colorbar;  
set(get(c6,'ylabel'),'string','Temperature [°C]','FontSize',axissize)  
view(0,270)  
title('Temperature Distribution (Time 2)', 'FontSize',titlesize)  
xlabel('x [pix]', 'FontSize',axissize)  
ylabel('y [pix]', 'FontSize',axissize)  
  
%Exporting of plots to LaTeX  
print(f1,'/Network/Servers/mlh34-0.ethz.  
ch/Volumes/01_MXS_RAID/01_StudentData/mheusser/Dropbox/experimentelle  
methoden/Schlieren Analysis/Report/pics/figure1','-dpng')  
print(f2,'/Network/Servers/mlh34-0.ethz.  
ch/Volumes/01_MXS_RAID/01_StudentData/mheusser/Dropbox/experimentelle  
methoden/Schlieren Analysis/Report/pics/figure2','-dpng')  
print(f3,'/Network/Servers/mlh34-0.ethz.  
ch/Volumes/01_MXS_RAID/01_StudentData/mheusser/Dropbox/experimentelle  
methoden/Schlieren Analysis/Report/pics/figure3','-dpng')  
print(f4,'/Network/Servers/mlh34-0.ethz.  
ch/Volumes/01_MXS_RAID/01_StudentData/mheusser/Dropbox/experimentelle  
methoden/Schlieren Analysis/Report/pics/figure4','-dpng')
```